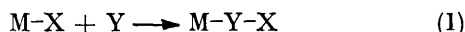


Photochemistry of Pentacarbonylmethylmanganese and Acetylpentacarbonylmanganese in Frozen Gas Matrices at 12 K. Infrared Spectroscopic Evidence for the Formation of Methyl- and Acetyl-tetracarbonylmanganese Species

By Terence M. McHugh and Antony J. Rest,* Department of Chemistry, The University, Southampton SO9 5NH

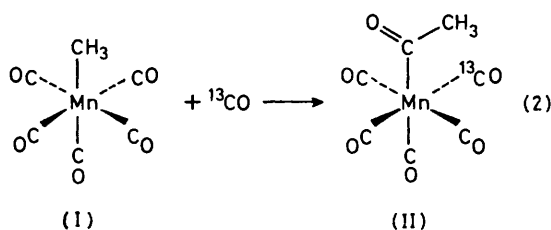
Infrared spectroscopic evidence is presented to show that on photolysis of $[\text{Mn}(\text{CO})_5\text{R}]$ ($\text{R} = \text{CH}_3$ or CH_3CO) complexes at high dilutions in Ar, CH_4 , and CO matrices at 12 K new species $[\text{Mn}(\text{CO})_4\text{R}]$ are produced. Carbon-13 labelling of CO and energy-factored force-field fitting was carried out for $[\text{Mn}(\text{CO})_5(\text{CH}_3)]$ and $[\text{Mn}(\text{CO})_4(\text{CH}_3)]$. For $[\text{Mn}(\text{CO})_4(\text{CH}_3)]$ the CH_3 ligand was shown to occupy an equatorial position in a trigonal-bipyramidal structure with C_2 symmetry. The observations of CO ejection, a new ketonic CO stretching band, and the formation of a species with a common $[\text{Mn}(\text{CO})_4]$ fragment from both $[\text{Mn}(\text{CO})_5(\text{CH}_3\text{CO})]$ and $[\text{Mn}(\text{CO})_5(\text{CH}_3^{13}\text{CO})]$, were interpreted as confirming the existence of the co-ordinatively unsaturated species $[\text{Mn}(\text{CO})_4(\text{CH}_3\text{CO})]$ as the intermediate in the decarbonylation reaction. Formation of *trans*- $[\text{Mn}(\text{CO})_4(\text{CH}_3^{13}\text{CO})]$ on reverse photolysis in experiments starting with *cis*- $[\text{Mn}(\text{CO})_4(\text{CH}_3^{13}\text{CO})]$ was interpreted as demonstrating that the $[\text{Mn}(\text{CO})_4(\text{CH}_3)]$ species is fluxional. The implications of fluxionality for the mechanism of the carbonylation reaction are discussed.

MANY organometallic reactions are of type (1) where M



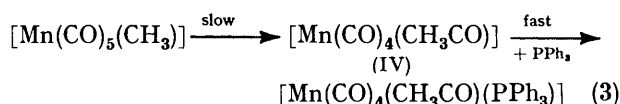
is a metal and its ancillary ligands, and X and Y are monoatomic or polyatomic species.¹ Such reactions are termed 'insertion' reactions although the word insertion does not have any literal mechanistic connotations. Some examples of M-X in equation (1) are: M-H, M-C, M-Halogen, M-O, and M-M and examples of Y are: CO, SO_2 , SO_3 , and olefins.

When Y is CO, the insertion reaction is described as a carbonylation reaction and for $[\text{Mn}(\text{CO})_5(\text{CH}_3)]$ it has been shown,² using ^{13}CO , that the inserting CO molecule is one which is already bound to the metal [equation (2)],



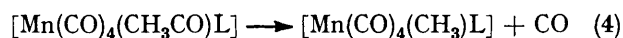
i.e. it is an intramolecular process. Several mechanistic studies on the carbonylation of $[\text{Mn}(\text{CO})_5\text{R}]$ promoted by CO,³ PPh_3 ,⁴ $\text{P}(\text{OR})_3$,⁵ and primary amines,⁴ *i.e.* equation (2) with ^{13}CO replaced by the promoting ligand, have been carried out. It was found^{6,7} that the acyl group and the promoting ligand were initially *cis* to each other, as in (II), but that in some cases the *cis* isomer isomerized to the *trans* isomer (III) so that a mixture of isomers was isolated from the reactions. Kinetic studies of the carbonylation of $[\text{Mn}(\text{CO})_5(\text{CH}_3)]$ promoted by PPh_3 showed⁸ that the reaction was first order in $[\text{Mn}(\text{CO})_5(\text{CH}_3)]$ but zero order in PPh_3 . This was interpreted as implying that the rate-determining step was the formation of a $[\text{Mn}(\text{CO})_4(\text{CH}_3\text{CO})]$ inter-

mediate which then rapidly reacted with PPh_3 [see equation (3)]. The intermediate (IV) was proposed⁹ to



have a square-pyramidal structure with the acetyl group in the apical (axial) position, *i.e.* a structure of type (V).

Three mechanisms can be considered for the carbonylation reaction: (i) alkyl migration, which involves the co-ordinated alkyl group moving on to an adjacent co-ordinated CO ligand to form the acyl group; (ii) CO insertion, literally a co-ordinated CO ligand moving to insert into the M-R bond; (iii) a co-operative movement of both co-ordinated R and CO groups. The reverse of carbonylation [equation (4)], which is termed de-

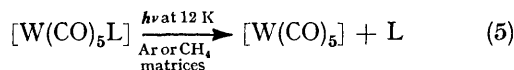


carbonylation, was shown to proceed by the same pathway as for carbonylation, in accordance with the principle of microscopic reversibility,¹⁰ *e.g.* $[\text{Mn}(\text{CO})_5(\text{CH}_3^{13}\text{CO})]$ gave exclusively *cis*- $[\text{Mn}(\text{CO})_4(\text{CH}_3^{13}\text{CO})]$ (Ia).² Furthermore, decarbonylation of *cis*- $[\text{Mn}(\text{CO})_4(\text{CH}_3^{13}\text{CO})-(\text{CH}_3\text{CO})]$ gave a *cis* : *trans* (2 : 1) mixture of $[\text{Mn}(\text{CO})_4-(\text{CH}_3^{13}\text{CO})(\text{CH}_3)]$ and this was taken as evidence for the methyl migration mechanism because the carbonyl insertion mechanism would have given no *trans* product and the co-operative mechanism would have afforded a higher proportion of the *cis* isomer.

In the search for intermediates in the substitution reactions of $[\text{Mn}(\text{CO})_5(\text{CH}_3\text{CO})]$ one possibility was thought to be a pyruvoyl species $[\text{Mn}(\text{CO})_4(\text{CH}_3\text{COCO})]$. However $[\text{Mn}(\text{CO})_5(\text{CH}_3\text{COCO})]$ was found to have a high kinetic stability and so it was considered more likely¹¹ that the intermediate was $[\text{Mn}(\text{CO})_4(\text{CH}_3\text{CO})]$.

The matrix isolation technique has been shown to be

an extremely powerful tool for investigating photochemical reactions and for characterising reactive species.¹² A variety of different carbonylmetal complexes have been investigated where ligand exchange takes place by a dissociative mechanism,¹² including the ejection of bulky ligands from complexes, *e.g.*¹³ equation (5) where L = pyridine, 3-bromopyridine, or



H₂S. In this paper we report on the species formed by photolysis of [Mn(CO)₅(CH₃)] and [Mn(CO)₅(CH₃CO)] in a variety of matrices at 12 K and we relate the results to the mechanisms of carbonylation and decarbonylation reactions. New ¹³C labelling studies show that the previous assignment¹⁴ of a trigonal-bipyramidal structure for [Mn(CO)₄(CH₃)] with the CH₃ ligand in the axial position, *i.e.* a C_{3v} molecule, was incorrect because of accidental superposition of terminal CO stretching fundamentals.

EXPERIMENTAL

Cryogenic temperatures (*ca.* 12 K) were obtained using a Displex CSA-202 closed-cycle helium refrigeration system (Air Products and Chemicals Inc.). Matrices of [Mn(CO)₅(CH₃)] (1:2 000 to 1:5 000) were prepared by 'pulsed' deposition¹⁵ of gas mixtures which were made up by standard manometric techniques. The complex [Mn(CO)₅(CH₃CO)], however, decomposed to give [Mn(CO)₅(CH₃)] in the gas phase and to prepare matrices of [Mn(CO)₅(CH₃CO)] and [Mn(CO)₅(CH₃¹³CO)] a slow deposition technique was used employing the apparatus described elsewhere.¹⁶ Vapour from the cooled solid (*ca.* -5 °C) was co-condensed with matrix gas onto the cold CsI or LiF window. Monomer isolation (*ca.* 1:2 000) was ensured by having a substantially higher gas flow for the host matrix gas than for the complex to be isolated. Deposition was monitored throughout by running i.r. spectra of the matrix and checking that the half-width at half-height of the terminal CO stretching bands did not exceed *ca.* 2 cm⁻¹.

Infrared spectra were recorded on a Grubb-Parsons Spectromajor grating spectrometer modified to have a grating change at 1 850 cm⁻¹ rather than at 2 000 cm⁻¹. Calibration in the 1 550–2 200 cm⁻¹ region was carried out regularly using the gas-phase absorptions of CO, DCl, and H₂O. Resolution was better than 1 cm⁻¹ and reproducibility of measurements was ±0.5 cm⁻¹. Ultra-violet-visible spectra were recorded on a Pye-Unicam SP1800B spectrometer.

The photolysis source was a medium-pressure mercury lamp (Philips HPK 125 W). Wavelength-selective photolysis was achieved by a combination of absorbing materials: filter A, λ < 280 and > 380 nm, quartz gas cell (pathlength 25 mm) containing Cl₂ gas (2 atm *); filter B, λ < 280 and > 500 nm, quartz gas cell containing Cl₂ gas + quartz gas cell (pathlength 25 mm) containing Br₂ gas (300 Torr); filter C, λ > 380 nm, quartz gas cell containing Cl₂ gas + a soda glass disc (thickness 5 mm); filter D, 280 < λ < 370 nm, quartz solution cell (pathlength 10 mm) containing

* Throughout this paper: 1 atm = 101 325 Pa; 1 Torr = (101 325/760) Pa; 1 eV ≈ 1.60 × 10⁻¹⁹ J.

Co[SO₄] and Ni[SO₄] (400 g l⁻¹ and 200 g l⁻¹ respectively) + Pyrex glass disc (thickness 7 mm). Additionally a Bausch and Lomb High Intensity Monochromator was used in conjunction with the medium-pressure mercury lamp. A low-pressure mercury lamp was also used.

Matrix gases (Ar, CH₄, CO) were of 'Grade X' purity (B.O.C. Ltd). Samples of [Mn(CO)₅(CH₃)], [Mn(CO)₅(CH₃CO)], and [Mn(CO)₅(CH₃¹³CO)] were prepared by standard reactions¹⁷ of CH₃I, CH₃COCl, and CH₃¹³COCl (91% ¹³C-enriched, B.O.C. Prochem Ltd.) respectively with NaMn(CO)₅, obtained by sodium amalgam reduction of [Mn₂(CO)₁₀] (Strem Chemicals Inc.), in tetrahydrofuran (thf) (Li[AlH₄] dried) at -40 °C. The solid products were isolated by removing the thf under vacuum, extracting the solid residue with n-pentane, and subsequently subliming the solid obtained by blowing off the n-pentane solvent with N₂. Samples were stored under N₂ at -20 °C and ¹H n.m.r. (Varian XL-100) was used to assess the purity of [Mn(CO)₅(CH₃CO)] (singlet at τ 7.44) and [Mn(CO)₅(CH₃¹³CO)] [*ca.* 90%, doublet at τ 7.44 with ²J(¹³CH) = 5 Hz; *ca.* 10%, singlet at τ 7.44], *i.e.* no peaks from [Mn(CO)₅(CH₃)]. The decomposition of [Mn(CO)₅(CH₃¹³CO)] in the gas phase thwarted attempts to make up matrix gas mixtures of this complex but afforded gas mixtures of *cis*-[Mn(¹²CO)₄(¹³CO)(CH₃)] and matrix gas ready for deposition onto the cold window.

RESULTS

The Isotopic Spectra of [Mn(CO)₅(CH₃)].—A gas-phase electron diffraction study of [Mn(CO)₅(CH₃)] has shown¹⁸ that the CO ligands adopt a C_{4v} geometry around the manganese and for such an arrangement three (2A₁ + E) i.r. active terminal CO stretching bands are expected.¹⁹ A typical i.r. spectrum for [Mn(CO)₅(CH₃)] in a matrix at 12 K is that of [Mn(CO)₅(CH₃)] in methane [Figure 1(a)]. As expected, three groups of bands are observed with splittings arising from matrix effects²⁰ (Table 1). The small doublet marked with an asterisk is due to a fundamental of *cis*-[Mn(¹²CO)₄(¹³CO)(CH₃)] (1a) occurring in natural abundance {see below for results with an authentic sample of *cis*-[Mn(¹²CO)₄(¹³CO)(CH₃)]}. In order to assign the structure of photolysis products arising from [Mn(CO)₅(CH₃)] and to investigate the possibility of fluxionality of the [Mn(CO)₄(CH₃)] species it was considered necessary to enrich the parent complex with ¹³CO and to analyse the spectra of [Mn(¹²CO)₅(CH₃)] [Figure 1(a)] and *cis*-[Mn(¹²CO)₄(¹³CO)(CH₃)] [Figure 2(a)] using an energy-factored force-field fitting procedure (see the Appendix of ref. 21 for details).

Use of the force constants obtained for [Mn(CO)₅(CH₃)] in solution²² allowed the band position of all the bands of [Mn(¹²CO)₅(CH₃)] and *cis*-[Mn(¹²CO)₄(¹³CO)(CH₃)] to be calculated.²¹ This calculation gave predicted spectra which were sufficiently similar to the observed spectra [Figures 1(a) and 2(a)] to enable all the bands to be assigned (see Appendix). The observed bands were subjected to a computer-based refinement (see the Appendix of ref. 21 for details) and the observed † and calculated wavenumbers are given in Table 2. The refined force constants for a CH₄ matrix are compared with those for a cyclohexane solution²² in Table 2.

Once the energy-factored force field was established

† In the event of matrix-split fundamentals it was found that a better fit could be obtained by inputting only the strongest contributing band.

for $[\text{Mn}^{(12}\text{CO})_5(\text{CH}_3)]$ and *cis*- $[\text{Mn}^{(12}\text{CO})_4(^{13}\text{CO})(\text{CH}_3)]$, the refined force constants were used to predict the position of the fundamentals for *trans*- $[\text{Mn}^{(12}\text{CO})_4(^{13}\text{CO})(\text{CH}_3)]$ (Ib). The calculations showed that of the three bands predicted

achieved with θ (see Appendix) = $96 \pm 2^\circ$ which is in good agreement with the electron diffraction determination (95°).¹⁸

*Photolysis of $[\text{Mn}(\text{CO})_5(\text{CH}_3)]$ and *cis*- $[\text{Mn}^{(12}\text{CO})_4(^{13}\text{CO})$ -*

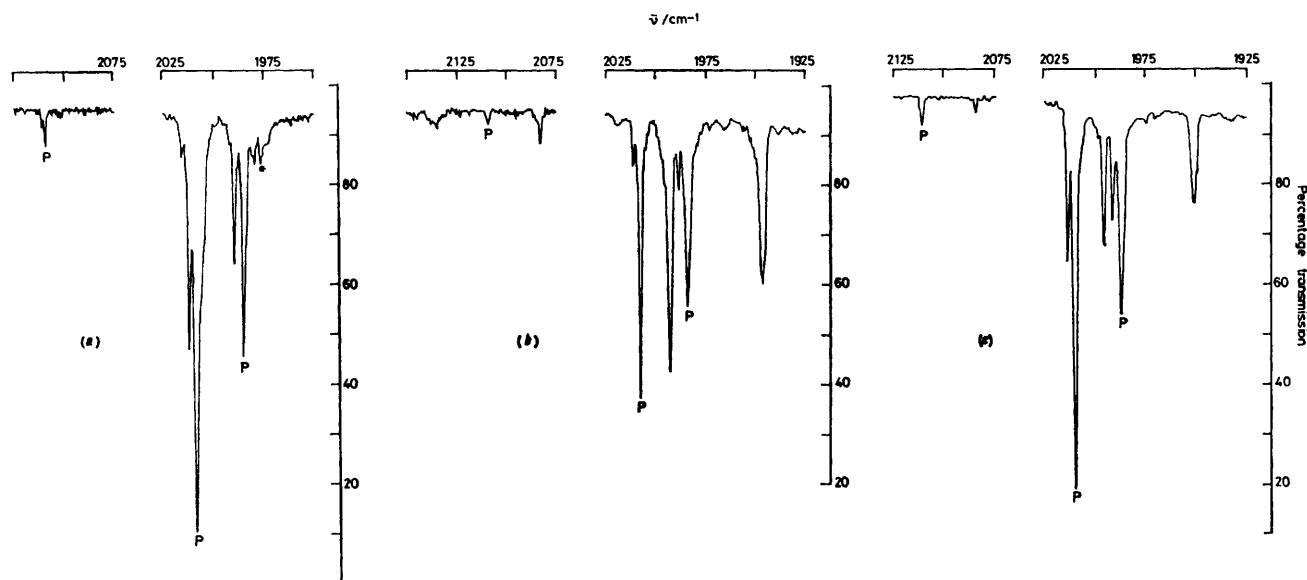


FIGURE 1 Infrared spectra from an experiment with $[\text{Mn}(\text{CO})_5(\text{CH}_3)]$ (bands marked P) isolated at high dilution in a CH_4 matrix at 12 K: (a) after deposition, (b) after 4 min photolysis using filter A, and (c) after further 30 min photolysis using filter C. Doublet marked with an asterisk is due to natural abundance *cis*- $[\text{Mn}^{(12}\text{CO})_4(^{13}\text{CO})(\text{CH}_3)]$

[2 106.7 (A_1), 2 012.8 (E), and 1 948.3 (A_1) cm^{-1}] the lower A_1 would be intense and would not be overlapped by other bands so that it could serve to indicate any isomerization in a cycle of forward and reverse photolysis. Additionally, the energy-factored force field allowed relative

(CH_3) in CH_4 , Ar, and CO Matrices.—Irradiation of $[\text{Mn}(\text{CO})_5(\text{CH}_3)]$ isolated at high dilution in a CH_4 matrix with u.v. light (filter A) corresponding to the electronic absorption bands (222s, 274w nm) which have been assigned²⁴ as metal→ligand charge-transfer bands (from

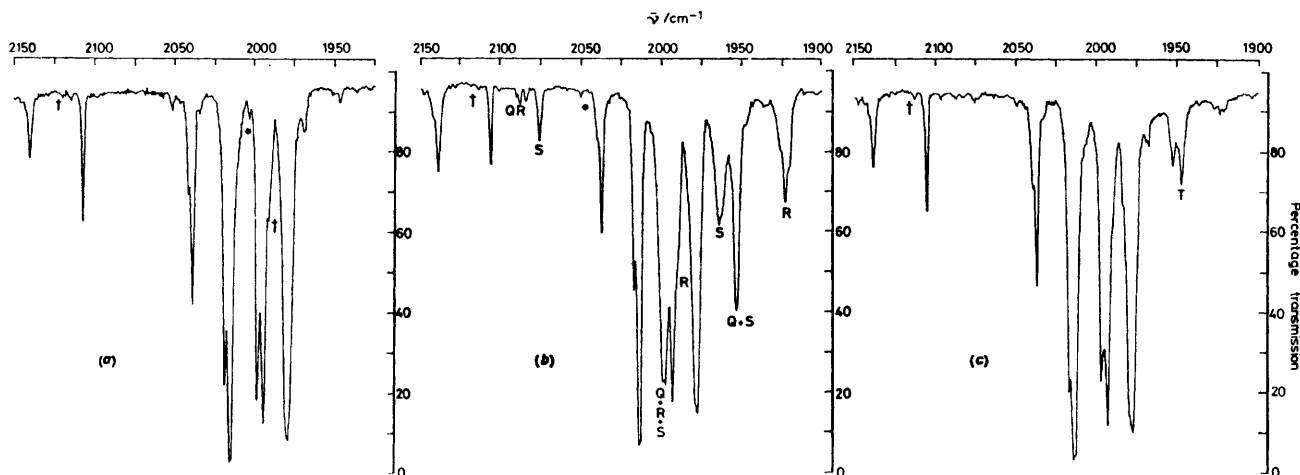


FIGURE 2 Infrared spectra from an experiment with *cis*- $[\text{Mn}^{(12}\text{CO})_4(^{13}\text{CO})(\text{CH}_3)]$ (Ia) isolated at high dilution in a CH_4 matrix at 12 K: (a) after deposition, (b) after 10 min photolysis using filter A, and (c) after further 90 min photolysis using filter C. Bands marked * and † are due to $[\text{Mn}(\text{CO})_5(\text{CH}_3^{13}\text{CO})]$ and $[\text{Mn}^{(12}\text{CO})_5(\text{CH}_3)]$ respectively. Product bands are identified with (VIII) (Q), (VIIIa) (R), and (VIIIb) (S). Doublet marked T is due to *trans*- $[\text{Mn}^{(12}\text{CO})_4(^{13}\text{CO})(\text{CH}_3)]$ (Ib)

band intensities to be determined (see the Appendix of ref. 21 for details) and compared with experimental band intensities (Table 2). A best fit, bearing in mind that the local oscillating dipole of a bond that does not lie on a rotational axis need not be collinear with that bond,²³ was

e_π molecular orbitals of the metal to π^* CO levels which are non-interacting with manganese orbitals) produced new bands [Figure 1(b)] at 2 136.2 cm^{-1} due to 'free' CO and at 2 086.9w, 1 997.4s, and 1 952.0m cm^{-1} (Table 1) with an associated decrease in the bands of $[\text{Mn}(\text{CO})_5(\text{CH}_3)]$.

TABLE 1

Band positions (cm^{-1})^a for $[\text{Mn}(\text{CO})_5(\text{CH}_3)]$ and $[\text{Mn}(\text{CO})_5(\text{CH}_3\text{CO})]$ complexes in the terminal and ketonic CO stretching region and their photoproducts in argon, methane, and carbon monoxide matrices at 12 K

Complex	$\nu(\text{CO})$	Ar	CH_4	CO
$[\text{Mn}(\text{CO})_5(\text{CH}_3)]$ C_{4v}	A_1	{ 2 116.2vw 2 114.5w	2 112.4w	2 112.3mw
	E	{ 2 020.5ms 2 015.6s	{ 2 016.4m 2 012.8s	{ 2 017.8ms 2 014.3s
	A_1	{ 1 998.8m 1 994.1ms	{ 1 993.5mw 1 988.0m	{ 1 989.9m 1 984.0w (sh)
	A_1	{ 2 094.1vw 2 091.5vw	2 086.9w	<i>b</i>
$[\text{Mn}(\text{CO})_4(\text{CH}_3)]$ C_{2v}	A_1	<i>c</i>	<i>c</i>	<i>c</i>
	B_1	{ 2 005.7ms 2 002.7s	1 997.4s	1 993.2s
	B_2	{ 1 960.8m 1 958.6m 1 955.0ms 1 953.1w (sh)	1 952.0m	1 954.7m
	A'	{ 2 122.7w 2 118.9w	{ 2 118.0w 2 116.9w	{ 2 121.9vw 2 118.7w
	A'	{ 2 066.3w 2 057.7mw 2 049.6w	{ 2 055.8mw 2 053.2mw 2 047.2w	{ 2 062.6w 2 054.7mw 2 047.5w
$[\text{Mn}(\text{CO})_5(\text{CH}_3\text{CO})]$ C_s	$A' \text{ }^d$	{ 2 030.1ms 2 021.2s 2 018.6ms	{ 2 026.2w 2 019.8ms 2 017.9ms	{ 2 026.7m 2 023.0ms 2 020.8s
	A''	{ 2 015.7s 2 013.1s	{ 2 015.6m 2 012.4ms	{ 2 019.1s 2 010.9s
	A'	{ 2 010.3s 2 005.6s	{ 2 007.6s 2 000.6s	{ 2 002.6ms
	A'	{ 1 665.3mw 1 652.4w	{ 1 661.1w 1 658.3w	{ 1 656.1mw 1 649.9w
	A'	2 087.5w	2 084.4w	<i>b</i>
	$A' \text{ }^e$	{ 1 996.8s 1 995.6s	{ 1 996.2m 1 992.0s	{ 1 996.7s 1 992.8s
	A''	{ 1 988.5m	1 988.5m	
	A'	1 955.4ms	1 948.0s	1 950.6ms
	A'	1 951.7m		
	A'	<i>f</i>	1 610.0vw	<i>f</i>
$[\text{Mn}(\text{CO})_4(\text{CH}_3\text{CO})]$ C_s	A'	2 087.5w	2 084.4w	<i>b</i>
	$A' \text{ }^e$	{ 1 996.8s 1 995.6s	{ 1 996.2m 1 992.0s	{ 1 996.7s 1 992.8s
	A''	{ 1 988.5m	1 988.5m	
	A'	1 955.4ms	1 948.0s	1 950.6ms
	A'	1 951.7m		

^a Relative intensities: vw = very weak, mw = medium weak, w = weak, m = medium, ms = medium strong, s = strong. Bands bracketed together arise from a single fundamental with matrix splitting unless otherwise stated. ^b Band obscured by matrix band of ^{13}CO . ^c Band obscured by the B_1 band of $[\text{Mn}(\text{CO})_4(\text{CH}_3)]$. ^d Multiplet comprises three matrix-split fundamentals. ^e Multiplet comprises two matrix-split fundamentals. ^f Band obscured by matrix-isolated H_2O band.

Selective photolysis with monochromatic light at 222 ± 10 nm or 274 ± 10 nm produced the same product bands although the efficiency of the photolysis was reduced. This was partly because of low lamp output at 222 nm and partly because of the lower extinction coefficient of the 274 nm absorption. Photolysis with an unmonochromated low-pressure mercury arc ($\lambda = 254$ nm) was found to be more efficient than a monochromated medium-pressure

TABLE 2

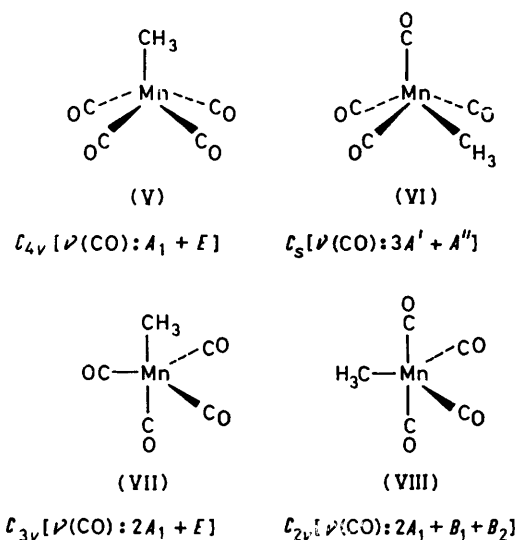
Observed^a and calculated^b band positions (cm^{-1}) and relative band intensities (in parentheses) for $[\text{Mn}(^{12}\text{CO})_5(\text{CH}_3)]$, *cis*- $[\text{Mn}(^{12}\text{CO})_4(^{13}\text{CO})(\text{CH}_3)]$, and *trans*- $[\text{Mn}(^{12}\text{CO})_4(^{13}\text{CO})(\text{CH}_3)]$ in the terminal CO stretching region for a CH_4 matrix at 12 K

Complex	$\nu(\text{CO})$	Observed	Calculated
$[\text{Mn}(^{12}\text{CO})_5(\text{CH}_3)]$ C_{4v} (I)	A_1	2 112.4 (2.2×10^{-2})	2 112.4 (2.4×10^{-2})
	B_2	<i>c</i>	2 041.5 ^e
	E	2 012.8 (1)	2 012.8 (1)
	A_1	1 988.0 (0.37)	1 987.0 (0.36)
<i>cis</i> - $[\text{Mn}(^{12}\text{CO})_4(^{13}\text{CO})(\text{CH}_3)]$ C_s rad ^{13}CO (Ia)	A'	2 105.1 (6×10^{-2})	2 105.2 (7×10^{-2})
	A'	2 035.3 (0.13)	2 035.5 (0.13)
	A''	2 012.8 (1)	2 012.8 (1)
	A'	1 992.2 (0.62)	1 992.1 (0.79)
	A'	1 976.3 (0.77)	1 975.9 (0.72)
<i>trans</i> - $[\text{Mn}(^{12}\text{CO})_4(^{13}\text{CO})(\text{CH}_3)]$ C_{4v} ax ^{13}CO (Ib)	A_1	<i>d</i>	2 106.7 (7×10^{-3})
	B_2	<i>c</i>	2 041.5 ^e
	E	<i>e</i>	2 012.8 (1)
	A_1	1 947.8 ^f	1 948.3 (0.34)

^a Strongest contributions to matrix-split bands (e.g. Table 1) were used to give band positions for the computer fitting. Combined intensities of matrix-split bands were obtained by weighing the area of chart paper covered by a particular fundamental (log mode spectra). ^b Refined energy-factored CO stretching and interaction force constants (N m^{-1}) as shown in (XIII) are: $K_{\text{ax}} = 1\ 627.8$, $K_{\text{rad}} = 1\ 682.1$, $k_t = 45.3$, $k_i = 21.8$, and $k_c = 36.9$; cf. corresponding force constants for cyclohexane solution (ref. 22): $K_{\text{ax}} = 1\ 622$, $K_{\text{rad}} = 1\ 681$, $k_t = 47.4$, $k_i = 24.3$, and $k_c = 31.0$ N m^{-1} . Bond moments used in calculations are shown in (XV). ^c Infrared inactive band. ^d Band too weak to be observed. ^e Band coincident with band of $[\text{Mn}(^{12}\text{CO})_5(\text{CH}_3)]$. ^f Calculation of ratio not possible (see text).

arc but it produced additional bands which may be attributed to secondary photolysis products, *i.e.* $[\text{Mn}(\text{CO})_n(\text{CH}_3)]$ where $n = 1-3$. A similar incidence of secondary photolysis was observed if the filter system B ($\lambda < 280$ and > 500 nm) was employed and this suggested that secondary photolysis was caused by short-wavelength radiation interacting with the primary product in the absence of an inhibiting process due to the primary product absorbing light in the wavelength range $380 < \lambda < 500$ nm. This was confirmed by subsequently irradiating with $\lambda > 380$ nm (filter C) radiation whereupon the primary product bands decreased and the bands of $[\text{Mn}(\text{CO})_5(\text{CH}_3)]$ increased in intensity [Figure 1(c)]. Annealing the matrix* also caused reversal of the primary forward photolysis. Since free CO was produced by u.v. photolysis of $[\text{Mn}(\text{CO})_5(\text{CH}_3)]$ at high dilutions and the relative intensities of the new bands, aside from secondary photolysis products, remained constant on varying the forward and reverse photolysis times, it seems probable that the species giving rise to the three new terminal CO stretching bands is $[\text{Mn}(\text{CO})_4(\text{CH}_3)]$.

Three of the possible four structures based on a square pyramid or a trigonal bipyramid [(V)–(VIII)] can give rise to three i.r. active terminal CO stretching fundamentals, one [(VII)] directly, as assigned in the preliminary report,¹⁴ and two [(VI) and (VIII)] as a result of accidental



band degeneracies. It should be noted that the solution i.r. spectrum of $[\text{Mn}(\text{CO})_4(\text{NO})]$ showed three terminal CO stretching fundamentals but a matrix isolation study²⁵ has shown that the complex has a C_{2v} structure (VIII) in accordance with X-ray crystallographic studies.²⁶ In order to distinguish between the three possibilities for $[\text{Mn}(\text{CO})_4(\text{CH}_3)]$ it was necessary to perform calculations of the band patterns for the various ¹³CO-enriched species.

Photolysis (filter A) of *cis*- $[\text{Mn}(\text{CO})_4(\text{CH}_3)(\text{CO})]$ in CH_4 produced new absorptions at 2 086.9w, 2 082.1w, 2 075.1w, 1 997.4s (broad), 1 989.6mw (sh), 1 964.6m, 1 951.9s, and 1 922.3m cm^{-1} together with an increase in the intensity of the 2 136.2 cm^{-1} band [Figure 2(b)]. Interestingly, reversal with long-wavelength radiation (filter

*Allowing the matrix to warm up to the softening temperature by switching off the refrigerator and then cooling again to 12 K before recording a spectrum.

C) regenerated the parent molecule with the appearance of an additional band at 1 947.8 cm^{-1} [Figure 2(c)], which may be assigned to the lower A_1 mode of *trans*- $[\text{Mn}(\text{CO})_4(\text{CH}_3)]$ (see above, Table 2). The formation of the *trans* isomer on reversal is important to the discussion about the structural consequences of $[\text{Mn}(\text{CO})_4(\text{CH}_3)]$ as a reaction intermediate in substitution and carbonylation reactions because it means that the tetracarbonyl species is fluxional.

Eliminating structure (V) because it predicts only two i.r. active CO stretching bands for $[\text{Mn}(\text{CO})_4(\text{CH}_3)]$, consideration of the number of possibilities for $[\text{Mn}(\text{CO})_5(\text{CH}_3)(\text{CO})]$ allows distinctions to be made between structures (VI) (three isomers), (VII) (two isomers), and (VIII) (two isomers). Comparing the number of observed bands with those expected for the isomers of (VI) (eight *versus* twelve respectively) it appears that an excessive number of accidental degeneracies would be required in order to match the observed band pattern. Furthermore, attempts to fit the observed band positions with combinations of band positions for the isomers of structure (VI) failed to converge and the predicted intensity patterns also failed to correlate with that observed. Structure (VII) cannot be discounted immediately on the basis of the number of bands predicted for the mono-enriched isomers but it too failed to allow exact band fitting and produced erroneous intensity ratios. The C_{2v} structure (VIII) however refined satisfactorily and predicted intensity ratios comparable with those observed (Table 3). It seems probable, therefore, that $[\text{Mn}(\text{CO})_4(\text{CH}_3)]$ adopts structure (VIII). For such a structure the bond dipole moment derivatives gave values for the $\text{OC}_{\text{eq}}-\text{Mn}-\text{CO}_{\text{eq}}$ and $\text{OC}_{\text{ax}}-\text{Mn}-\text{CO}_{\text{ax}}$ angles of 123 ± 2 and $179 \pm 3^\circ$.

Results using an argon matrix paralleled those for methane described above although there were small differences in band position and splitting patterns (Table 1), which may be attributed to differing matrix solvent effects and packing. Photolysis efficiency for the formation of $[\text{Mn}(\text{CO})_4(\text{CH}_3)]$ was also reduced in argon compared to methane, in agreement with the report²⁷ that the photolysis of $[\text{Mo}(\text{CO})_6]$ using an unfiltered mercury arc was substantially more efficient in a CH_4 matrix than in Ar. Subsequent relative quantum yield measurements showed²⁸ that the difference originated in the competing recombination of $[\text{Mo}(\text{CO})_5]$ with photo-ejected CO which is less efficient for CH_4 than Ar rather than intrinsic differences in the quantum yield for the destruction of $[\text{Mo}(\text{CO})_6]$. Interestingly, photolysis of $[\text{Mn}(\text{CO})_5(\text{CH}_3)]$ in CO matrices also resulted in the formation of $[\text{Mn}(\text{CO})_4(\text{CH}_3)]$ (Table 1) in accordance with the formation of $[\text{Cr}(\text{CO})_5]$ from $[\text{Cr}(\text{CO})_6]$ in CO matrices.²⁹ In view of the success of CO as a reactive matrix, *e.g.* formation of $[\text{Co}(\text{CO})_4]$ from $[\text{Co}(\text{CO})_3(\text{NO})]$,³⁰ this result would seem to cast doubts on the claim by Ogilvie³¹ to convert $[\text{Mn}(\text{CO})_5(\text{CH}_3)]$ to an acetylcarbonylmanganese species $[\text{Mn}(\text{CO})_n(\text{CH}_3\text{CO})]$ in an argon matrix. The failure to form $[\text{Mn}(\text{CO})_5(\text{CH}_3\text{CO})]$ from $[\text{Mn}(\text{CO})_5(\text{CH}_3)]$ in a CO matrix is consistent with the fact that a considerable pressure of CO (300 atm) is required for the conversion in the gas phase.³²

Photolysis of $[\text{Mn}(\text{CO})_5(\text{CH}_3\text{CO})]$ and $[\text{Mn}(\text{CO})_5(\text{CH}_3^{13}\text{CO})]$ in CH_4 , Ar, and CO Matrices.—The i.r. spectrum of $[\text{Mn}(\text{CO})_5(\text{CH}_3\text{CO})]$ isolated at high dilution in a CH_4 matrix is shown in Figure 3(a). Comparison of the spectrum with that of $[\text{Mn}(\text{CO})_5(\text{CH}_3)]$ [Figure 1(a)] indicates that the acetyl group has lowered the local symmetry of the $[\text{Mn}(\text{CO})_5]$ fragment from C_{4v} to C_s with the high degree of

splitting resulting from either two orientations of the Mn-CO-C plane with respect to the $\text{Mn}(\text{CO})_4$ plane or a range of orientations corresponding to a freely rotating acetyl group but trapped out during deposition. The electronic

ketonic CO stretching mode. Selective photolysis with monochromated light failed to eliminate the formation of $[\text{Mn}(\text{CO})_5(\text{CH}_3)]$. Attempts to reverse the primary photolysis using long-wavelength radiation (filter C) were un-

TABLE 3

Observed ^a and calculated ^b band positions (cm^{-1}) and relative band intensities (in parentheses) for ¹³CO-enriched $[\text{Mn}(\text{CO})_4(\text{CH}_3)]$ species in the terminal CO stretching region for a CH_4 matrix

Complex	$\nu(\text{CO})$	Observed	Calculated
$[\text{Mn}(\text{CO})_4(\text{CH}_3)] C_{2v}$ (VIII)	A_1	2 086.9 (0.07)	2 087.0 (0.07) ^e
	A_1		1 999.9 (0.15)
	B_1	1 997.4 (1)	1 997.4 (0.85)
	B_2	1 952.0 (0.76)	1 951.6 (0.76) ^e
	A'	2 082.1 (0.06)	2 081.9 (0.08) ^e
$[\text{Mn}(\text{CO})_3(\text{CO})(\text{CH}_3)] C_s$ eq ¹³ CO(VIIIa)	A'	1 997.4 (f)	1 997.4 (1.28) ^e
	A'	1 989.6 (f)	1 989.6 (0.33) ^e
	A''	1 922.3 (1)	1 922.9 (1) ^e
	A'	2 075.1 (0.17)	2 075.3 (0.18) ^e
	A''		1 999.4 (0.44) ^e
$[\text{Mn}(\text{CO})_3(\text{CO})(\text{CH}_3)] C_s$ ax ¹³ CO(VIIIb)	A'	1 964.6 (1.2)	1 964.7 (0.9) ^e
	A'	1 951.9 (1.16) ^h	1 951.6 (1.15) ^e

^a Weighted averages of matrix-split bands (e.g. Table 1) were used to give band positions for the computer fitting. ^b Refined energy-factored CO-stretching and -interaction force constants (N m^{-1}) as shown in (XIV) are: $K_{ax} = 1\ 664.1$, $K_{eq} = 1\ 599.0$, $k_t = 52.2$, $k_l = 60.3$, and $k_o = 33.0$. Bond moments used in calculations are shown in (XVI). ^c Estimated taking the total intensity of the 1 999.9 and 1 997.4 cm^{-1} band as unity. ^d Obscured by 1 997.4 cm^{-1} band. Intensity included in the intensity of the 1 997.4 cm^{-1} band. ^e Calculated assuming a 1 : 1 mixture of axially and equatorially ¹³CO-substituted $[\text{Mn}(\text{CO})_4(\text{CH}_3)]$. The intensity of the 1 922.9 cm^{-1} band was set at 1 and the relative band intensities for the remaining bands were calculated with respect to it. The calculated intensities of these two isotopically enriched species are not directly comparable to those of $[\text{Mn}(\text{CO})_4(\text{CH}_3)]$. ^f Obscured by 1 992.1 cm^{-1} band of *cis*- $[\text{Mn}(\text{CO})_4(\text{CO})(\text{CH}_3)]$. ^g Observed as a broadening of the 1 997.4 cm^{-1} band. ^h Observed ratio corrected for contribution from 1 951.6 cm^{-1} band of (VIII).

spectrum showed a strong absorption at $\lambda < 240$ nm together with a point of inflection at 288 nm and a weak band at 334 nm.

Photolysis with $280 < \lambda < 370$ nm radiation (filter D)

successful producing only an increase in the intensities of the bands due to $[\text{Mn}(\text{CO})_5(\text{CH}_3)]$ corresponding to the decrease in the primary photo-product bands.

The detection of new terminal CO stretching absorptions

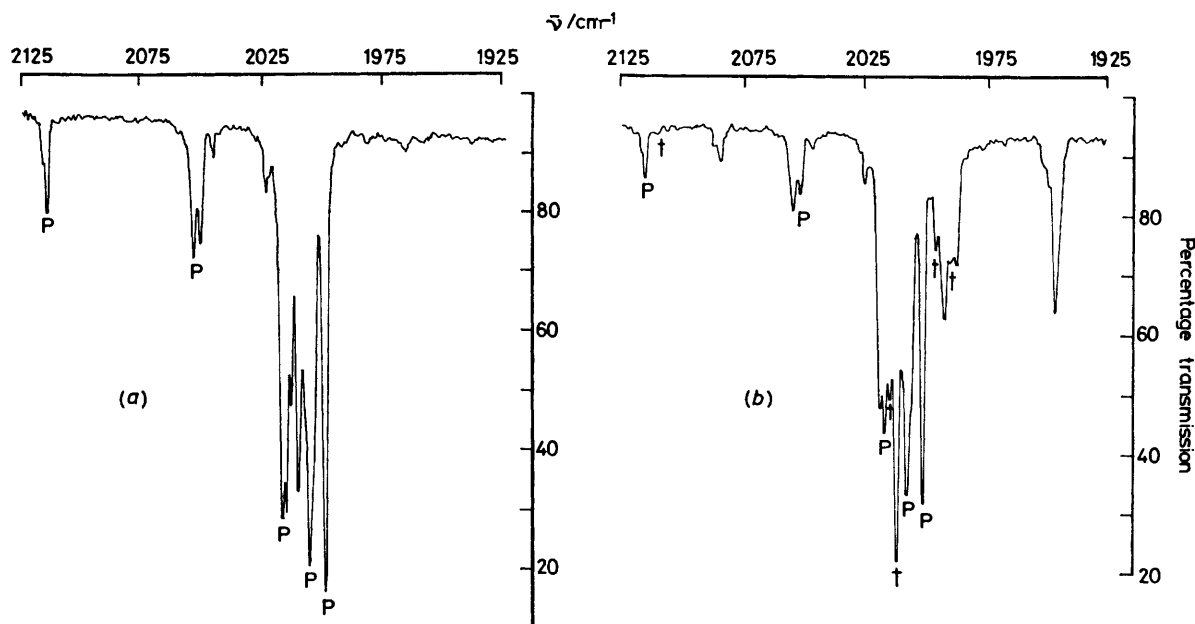


FIGURE 3 Infrared spectra from an experiment with $[\text{Mn}(\text{CO})_5(\text{CH}_3\text{CO})]$ (bands marked P) isolated at high dilution in a CH_4 matrix at 12 K: (a) after deposition and (b) after 3 min photolysis using filter D. Bands marked with a dagger are due to $[\text{Mn}(\text{CO})_5(\text{CH}_3)]$

produced new bands associated with $[\text{Mn}(\text{CO})_5(\text{CH}_3)]$ (marked †) and CO together with four additional bands at 2 084.4w, 1 992.0m, 1 948.0m, and 1 610.0vw cm^{-1} [Figure 3(b)], of which the 1 610.0 cm^{-1} band can be assigned as a

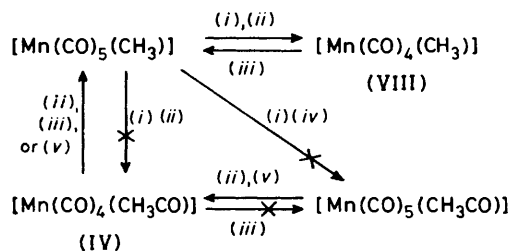
that cannot be assigned to $[\text{Mn}(\text{CO})_5(\text{CH}_3)]$ or $[\text{Mn}(\text{CO})_4(\text{CH}_3)]$ coupled with the observation of a new ketonic CO stretching band strongly suggests that the new species formed on u.v. photolysis of $[\text{Mn}(\text{CO})_5(\text{CH}_3\text{CO})]$ is $[\text{Mn}$ -

(CO)₄(CH₃CO)]. Photolysis of [Mn(CO)₅(CH₃¹³CO)] in CH₄ with filter D produced *cis*-[Mn(¹²CO)₄(¹³CO)(CH₃)] and three terminal CO stretching bands occurring at the *same* wavenumbers as those of [Mn(CO)₄(CH₃¹²CO)]. The ketonic CO stretching band of [Mn(CO)₄(CH₃¹³CO)] could not be observed due to masking in the 1 580—1 610 cm⁻¹ region by bands arising from matrix isolated water. The fact that both [Mn(CO)₅(CH₃¹²CO)] and [Mn(CO)₅(CH₃¹³CO)] yield the *same* wavenumbers for the terminal CO stretching fundamentals of the new species is conclusive evidence for the retention of the acetyl moiety and the formulation of the new species as [Mn(CO)₄(CH₃CO)]. The detailed structure of [Mn(CO)₄(CH₃CO)] was not determined because of the thermal and photochemical instability of [Mn(CO)₅(CH₃CO)] under conditions which would have allowed ¹³CO exchange to form [Mn(¹²CO)_n(¹³CO)_{5-n}(CH₃CO)]. A possible route to [Mn(¹²CO)_n(¹³CO)_{5-n}(CH₃CO)] *via* [Mn₂(¹²CO)_n(¹³CO)_{10-n}] was not attempted. Additionally, conversion from [Mn(CO)₅(CH₃CO)] to [Mn(CO)₄(CH₃CO)] always resulted in formation of [Mn(CO)₅(CH₃)] and it would probably not have been possible to unscramble the complex band pattern that would have been produced. However the relative intensities of the bands of [Mn(CO)₄(CH₃CO)] and those of [Mn(CO)₄(CH₃)] are very similar and on this basis [Mn(CO)₄(CH₃CO)] is tentatively assigned as having the C_{2v} structure of type (VIII) in common with other [Mn(CO)₄X] (X = Cl, Br, or I) species.²¹

Analogous results were obtained for Ar and CO matrices (Table I), although the matrix splittings were different and the rate of conversion to [Mn(CO)₄(CH₃CO)] and [Mn(CO)₅(CH₃)] was slower.

DISCUSSION

The photoreactions of [Mn(CO)₅(CH₃)] and [Mn(CO)₅(CH₃CO)] at high dilution in frozen gas matrices are summarized in Scheme 1. They are discussed in relation

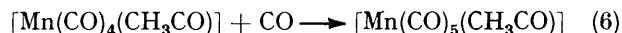


SCHEME 1 (i) $h\nu$ (filter A); (ii) CH₄, Ar, CO; (iii) $h\nu$ (filter C); (iv) CO; (v) $h\nu$ (filter D)

to the overall mechanism of decarbonylation-carbonylation and also to isomerizations occurring during the reactions as a result of the possible fluxionality of the five-co-ordinate [Mn(CO)₄(CH₃)] species.

The Overall Mechanism of Decarbonylation-Carbonylation.—In accordance with the principle of microscopic reversibility,¹⁰ decarbonylation of [Mn(CO)₅(CH₃CO)] should occur *via* the reverse of the carbonylation reaction, *i.e.* dissociative loss of CO followed by a methyl migration on to the vacant co-ordination site at the metal. The formation of [Mn(CO)₅(CH₃)] from [Mn(CO)₅(CH₃CO)] *via* [Mn(CO)₄(CH₃CO)], even when CO is used as a matrix, strongly supports the proposed mechanism for decarbonylation. The irreversibility of

the primary photolysis step for [Mn(CO)₅(CH₃CO)] in Scheme 1 can be accounted for in two ways. (i) The activation energy barrier for the process (6) may be



higher than that for (7) since the latter process has no orientation barrier because it is an intramolecular process. (ii) Although [Mn(CO)₅(CH₃CO)] has been shown to be thermodynamically more stable than [Mn(CO)₅(CH₃)],¹¹ the overall energy change for sequences of reactions from [Mn(CO)₅(CH₃CO)] to [Mn(CO)₅(CH₃)] (Scheme 1) may well be more favourable than the process shown in equation (6) because the former produces two stable molecules whereas the latter produces only one.

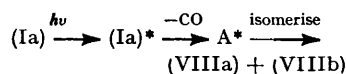
Surprisingly, no evidence could be found for the formation of [Mn(CO)₄(CH₃CO)] on photolysis of [Mn(CO)₅(CH₃)] (Scheme 1) even in a pure CO matrix. It may well be that [Mn(CO)₄(CH₃)] is thermodynamically more stable than [Mn(CO)₄(CH₃CO)] or, alternatively, that there is a higher activation energy required for the formation of [Mn(CO)₄(CH₃CO)]. Once again the broadness of the electronic absorption bands and the ready photochemical conversion of [Mn(CO)₄(CH₃CO)] to [Mn(CO)₅(CH₃)] may have precluded the necessary wavelength-selective photolysis. However, it should be noted that carbonylation of [Mn(CO)₅(CH₃)] requires a high pressure of CO (300 atm) which indicates that the reaction is not particularly favourable.³²

The Isomerization of *cis*-[Mn(¹²CO)₄(¹³CO)(CH₃)] (Ia) and the Fluxionality of [Mn(CO)₄(CH₃)].—The generation of *trans*-[Mn(¹²CO)₄(¹³CO)(CH₃)] (Ib) on long-wavelength photolysis of a mixture of equatorially and axially ¹³CO-substituted [Mn(CO)₄(CH₃)] [(VIIIa) and (VIIIb)] implies fluxionality in one or more of the photoreactions. A similar observation has been made by Poliakoff³³ who found that u.v. photolysis of *trans*-[W(¹²CO)₄(¹³CO)(CS)] yielded a mixture of tetracarbonyl isomers based on a square-pyramidal structure, *i.e.* (V) or (VI), that could only be rationalised in terms of a *trans*→*cis* isomerization of the CS and ¹³CO ligands. Furthermore, the experiments indicated³³ that the isomerization occurred from an excited state of the tetracarbonyl. Although discounted for *trans*-[W(¹²CO)₄(¹³CO)(CS)],³¹ it is possible to argue that the isomerization may occur prior to the ejection of a ¹²CO or ¹³CO ligand from *cis*-[Mn(¹²CO)₄(¹³CO)(CH₃)] (Ia). If this was so, however, it might be expected that some *trans*-[Mn(¹²CO)₄(¹³CO)(CH₃)] would be formed *prior* to irradiation with visible light but no evidence for this was found. It should be noted that stereochemical non-rigidity for ¹³C¹⁸O enriched [W(CO)₅{P(OCH₃)₃}] has been found³⁴ to occur by a process which did not involve the loss of either CO or P(OCH₃)₃ ligands, *i.e.* an intramolecular arrangement.

The u.v. photolysis of (Ia) may be represented as in Scheme 2. The nature of the species A* warrants

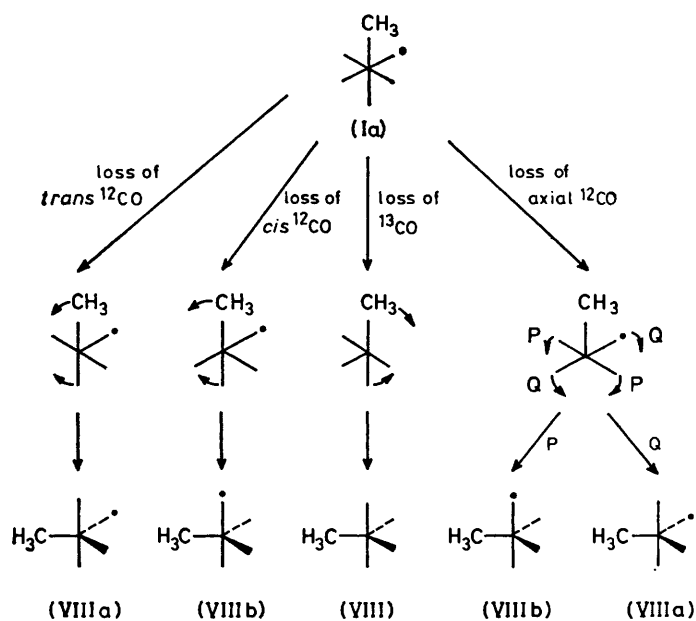
discussion which relates to the distribution of isomers found in solution carbonylation and decarbonylation reactions, *e.g.* equations (2)–(4). Considering loss of ^{12}CO ligands *cis* and *trans* to the ^{13}CO in the equatorial plane and the loss of the axial ^{12}CO ligand, followed by a simple distortion of bond angles of the type associated with Berry pseudo-rotation³⁵ the possible routes to (VIII), (VIIIa), and (VIIIb) from (Ia) can be represented as in Scheme 3.

Assuming stereochemical rigidity, the processes outlined in Scheme 3 would predict the ratio of (VIII) : (VIIIa) : (VIIIb) as 2 : 3 : 5 whereas the observed ratio of (VIIIa) : (VIIIb) is 1 : 1. Allowing (VIIIa) and (VIIIb) to be fluxional rationalises the situation because (VIIIa) and (VIIIb) can be easily interconverted by one consecutive trigonal bipyramidal (tbp) \rightarrow square pyramidal



SCHEME 2 (Ia)* and A* are excited-state species

(spy) \rightarrow trigonal bipyramidal interconversion, *i.e.* one Berry³⁵ pseudo-rotation (Scheme 4). Very few such interconversions are required to produce a purely statistical ratio of (VIIIa) to (VIIIb), *i.e.* 1 : 1. Furthermore the

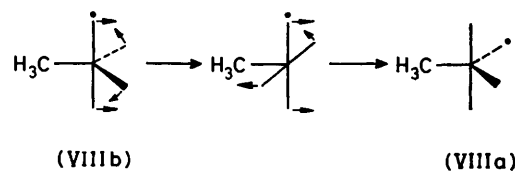


SCHEME 3 The dot represents a ^{13}CO ligand

mechanism accounts for the formation of *trans*-[Mn(^{12}CO)₄(^{13}CO)(CH₃)] on recombination* of the five-coordinate fragments with photo-ejected CO. A possible series of processes by which the *trans*-[Mn(^{12}CO)₄(^{13}CO)(CH₃)] species can be generated is shown in Scheme 5.

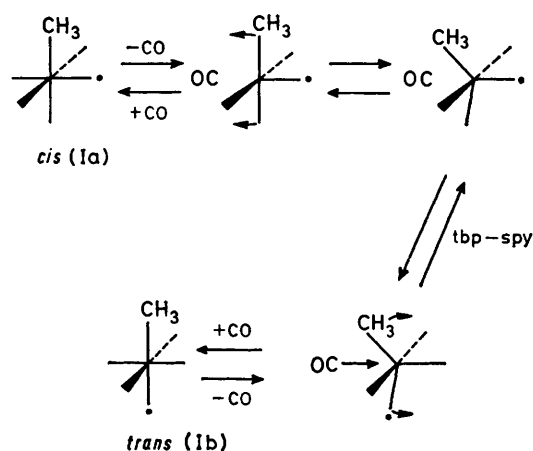
* For the purposes of considering such recombinations, any photoejected CO molecule is assumed to be in a position where it still occupies a well defined site close to the [Mn(CO)₄(CH₃)] species rather than having diffused away into the matrix.³⁶ This assumption is justified because the forward photolysis time to produce [Mn(CO)₄(CH₃)] species in all cases was short (*ca.* 5 min).

It should be noted that the reorientation is probably the combined result of the *tbp*–*spy* interconversions and restricted thermal motion of both the fragment and the



SCHEME 4 The dot represents a ^{13}CO ligand

photo-ejected CO. Whether the interconversions occur from an excited electronic state or from a vibrationally excited ground state is uncertain. The presence of a significant † amount of *trans*-[Mn(^{12}CO)₄(^{13}CO)(CH₃)] after reversal suggests that several consecutive trigonal-



SCHEME 5 The dot represents a ^{13}CO ligand

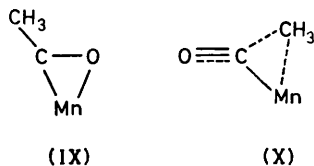
bipyramidal–square-pyramidal rearrangements occur between the ejection of CO from the *cis*-[Mn(^{12}CO)₄(^{13}CO)(CH₃)] parent complex and the arrival of product species in vibrational ground states since many of the available pathways leave the [Mn(^{12}CO)₃(^{13}CO)(CH₃)] fragment and the CO ligand in orientations that can only regenerate *cis*-[Mn(^{12}CO)₄(^{13}CO)(CH₃)]. This suggests that there is a small activation energy barrier for the isomerization process so that some of the earlier mechanistic conclusions² based on the distribution of ^{13}CO during reactions may need to be reinvestigated in the light of the fluxionality of [Mn(CO)₄(CH₃)] shown here. Such fluxionality of co-ordinatively unsaturated inter-

† Unfortunately it was not possible to calculate to any significant degree of accuracy the relative amounts of *cis* : *trans*-[Mn(^{12}CO)₄(^{13}CO)(CH₃)] regenerated on a long-wavelength photolysis because the only band observable for the *trans* isomer is that at 1 947.8 cm⁻¹ which, for any comparison to be meaningful on the basis of bond dipole moments and extinction coefficients, requires comparison with the 1 992 cm⁻¹ band of the *cis* isomer. However, the absorption at 1 992 cm⁻¹ incorporates contributions from [Mn(CO)₅(CH₃)] and *cis*-[Mn(^{12}CO)₄(^{13}CO)(CH₃)] as well as any unreversed (VIII), (VIIIa), and (VIIIb). The other possibility would be comparison of the highest wavenumber fundamentals but these are so weak (Table 2) that again any comparison is bound to be very inaccurate.

mediates is beginning to be taken into account in solution kinetic studies.^{37,38} Even co-ordinatively saturated species, *e.g.* $[\text{W}(\text{CO})_5\{\text{P}(\text{OCH}_3)_3\}]$, have been shown³⁴ to undergo intramolecular rearrangement without loss of any ligands.

The Structures of $[\text{Mn}(\text{CO})_4(\text{CH}_3)]$ and $[\text{Mn}(\text{CO})_4(\text{CH}_3\text{CO})]$.—Matrix isolation studies have shown that $[\text{Mn}(\text{CO})_4(\text{CH}_3)]$, and probably also $[\text{Mn}(\text{CO})_4(\text{CH}_3\text{CO})]$, adopts a C_{2v} trigonal-bipyramidal structure (VIII) with the alkyl or acetyl group in the equatorial plane. This is in accordance with the structure adopted by $[\text{Mn}(\text{CO})_4\text{X}]$ species (X = Cl, Br, or I) in low-temperature matrices²¹ and the structure favoured for $[\text{Mn}(\text{CO})_4\text{Br}]$ in molecular-orbital calculations.³⁹ In these calculations a square-pyramidal geometry of type (VI) was found to be the next lowest energy configuration but the energy separation between types (VIII) and (VI) was not so large as to prevent Berry-type interconversion between the two structures.³⁹ In other molecular-orbital calculations⁴⁰ on the isomers of $[\text{Mn}(\text{CO})_4(\text{CH}_3\text{CO})]$, however, it was found that the acetyl group preferred the basal site in a square-pyramidal structure of type (VI) to the extent of 0.65 eV, the difference between the Br and CH_3CO ligands being the smaller π -donating component of the CH_3CO group.⁴⁰ Kinetic studies also favour a rigid square-pyramidal structure of type (VI) for $[\text{Mn}(\text{CO})_4(\text{CH}_3\text{CO})]$ unequivocally⁴¹ but these studies may not have taken sufficient account of the fluxionality of the type demonstrated in this work or in the intramolecular rearrangement of $[\text{W}(\text{CO})_5\{\text{P}(\text{OCH}_3)_3\}]$.³⁴

Other structural possibilities to consider are the dihapto-acetyl structure (IX) and a transition-state



structure (X) which allows the methyl group to migrate in the decarbonylation or carbonylation steps. Structural evidence for dihapto-acyls is steadily accumulating⁴²⁻⁴⁶ but molecular-orbital calculations showed⁴⁰ that such an interaction was less favourable for $[\text{Mn}(\text{CO})_4(\text{CH}_3\text{CO})]$ than for $[\text{M}(\eta\text{-C}_5\text{H}_5)_2(\text{CH}_3)(\text{CH}_3\text{CO})]$ complexes (M = Ti or Zr).⁴² The large shift (*ca.* 50 cm^{-1} , Table I) of the acetyl stretching vibration to lower wavenumbers for the co-ordinatively unsaturated species $[\text{Mn}(\text{CO})_4(\text{CH}_3\text{CO})]$ implies a weakening in the ketonic CO bond and as such is more consistent with (IX) than (X) although either (IX) or (X) could be responsible for the *cis* labilising effect of the acetyl group in $[\text{Mn}(\text{CO})_5(\text{CH}_3\text{CO})]$.⁴⁷

Conclusions.—Matrix isolation studies have shown that $[\text{Mn}(\text{CO})_4\text{R}]$ species (R = CH_3 or CH_3CO) adopt a C_{2v} trigonal-bipyramidal structure (VIII) with the R group in the equatorial plane. It seems likely there-

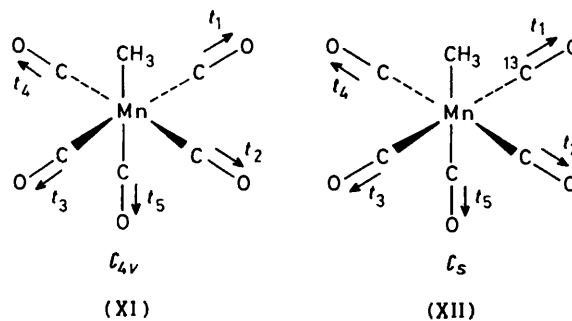
fore, that $[\text{Mn}(\text{CO})_4\text{H}]$,⁴⁸ which, like $[\text{Mn}(\text{CO})_4(\text{CH}_3)]$,¹⁴ was assigned a structure of type (VII) * on the basis of *three* i.r. active CO stretching modes, also has a structure of type (VIII), *i.e.* $[\text{Mn}(\text{CO})_4\text{X}]$ species (X = Cl, Br, I, CH_3 , CH_3CO , or H) have a common structure.

The observation of $[\text{Mn}(\text{CO})_4(\text{CH}_3\text{CO})]$ on photolysis of $[\text{Mn}(\text{CO})_5(\text{CH}_3\text{CO})]$ adds weight to the dissociative mechanism proposed² for the decarbonylation reaction proceeding by a methyl migration.

Experiments with *cis*- $[\text{Mn}^{12}\text{CO}_4(^{13}\text{CO})(\text{CH}_3)]$ have shown that $[\text{Mn}(\text{CO})_4(\text{CH}_3)]$ is fluxional. It is important, therefore, when proposing reaction mechanisms involving co-ordinatively unsaturated species that aspects of fluxionality are fully taken into consideration. This may mean that earlier interpretations of the results from kinetic studies, *e.g.* decarbonylation of *cis*- $[\text{Mn}^{12}\text{CO}_4(^{13}\text{CO})(\text{CH}_3\text{CO})]$,² need to be reinvestigated.

APPENDIX

The internal co-ordinates for the CO stretching fundamentals of $[\text{Mn}(\text{CO})_5(\text{CH}_3)]$ and *cis*- $[\text{Mn}^{12}\text{CO}_4(^{13}\text{CO})(\text{CH}_3)]$ are defined as shown in (XI) and (XII). These



internal co-ordinates generate the symmetry co-ordinates shown below.

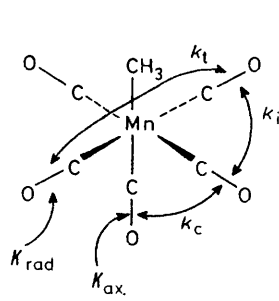
$[\text{Mn}(\text{CO})_5(\text{CH}_3)]$	<i>cis</i> - $[\text{Mn}^{12}\text{CO}_4(^{13}\text{CO})(\text{CH}_3)]$
$A_1: \frac{1}{2}(t_1 + t_2 + t_3 + t_4)$	$A': t_1$
$A_1: t_5$	$A': \sqrt{\frac{1}{2}}(t_2 + t_4)$
$E: \left. \begin{array}{l} \sqrt{\frac{1}{2}}(t_1 - t_3) \\ \sqrt{\frac{1}{2}}(t_2 - t_4) \end{array} \right\}$	$A': t_3$
	$A'': \sqrt{\frac{1}{2}}(t_2 - t_4)$
	$A': t_5$

Examination of the symmetry co-ordinates reveals that the A'' vibration of *cis*- $[\text{Mn}^{12}\text{CO}_4(^{13}\text{CO})(\text{CH}_3)]$ has the same co-ordinates as one of the degenerate E co-ordinates of $[\text{Mn}(\text{CO})_5(\text{CH}_3)]$ and accordingly the 2012.8 cm^{-1} fundamental of *cis*- $[\text{Mn}^{12}\text{CO}_4(^{13}\text{CO})(\text{CH}_3)]$ was assigned as having A'' symmetry. Assigning the upper A_1 vibration of $[\text{Mn}(\text{CO})_5(\text{CH}_3)]$ as deriving from the equatorial symmetric CO stretch $[\frac{1}{2}(t_1 + t_2 + t_3 + t_4)]$, 2112.4 cm^{-1} and the lower A_1 mode as deriving from the axial CO stretch (t_5 , 1988.0 cm^{-1}), it is expected that one A' band of *cis*- $[\text{Mn}^{12}\text{CO}_4(^{13}\text{CO})(\text{CH}_3)]$ should occur near 1988.0 cm^{-1} (t_5). Actually this band is observed at 1992.2 cm^{-1} because of mixing with the other A' modes. Another A' mode $[\sqrt{\frac{1}{2}}(t_2 + t_4)]$ should occur close to the A_1 symmetric

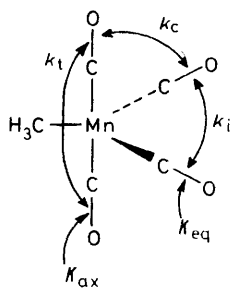
* Preliminary results of a further investigation of $[\text{Mn}(\text{CO})_4\text{H}]$ favour a structure of type (VI) but there may also be more than one isomer present.⁴⁹ Work is continuing on this problem.⁵⁰

stretch of $[\text{Mn}(\text{CO})_5(\text{CH}_3)]$ ($2.112.5 \text{ cm}^{-1}$), *i.e.* the band at 2105.1 cm^{-1} . This leaves two A' modes, one of which derives from the ^{13}CO (t_1) and this is expected to show a shift of *ca.* 40 cm^{-1} from the E mode of $[\text{Mn}(\text{CO})_5(\text{CH}_3)]$ in accordance with the Teller-Redlich product rule,¹⁹ *i.e.* the band at 1976.3 cm^{-1} (t_1), which leaves the 2035.3 cm^{-1} band as arising from the other symmetry co-ordinate (t_2).

The complete assignment of the bands allowed a complete determination of the energy-factored force field for $[\text{Mn}(\text{CO})_5(\text{CH}_3)]$.

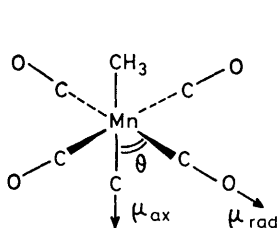


(XIII)

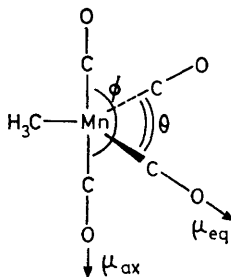


(XIV)

$(\text{CO})_5(\text{CH}_3)$. The energy-factored force constants for $[\text{Mn}(\text{CO})_5(\text{CH}_3)]$ and $[\text{Mn}(\text{CO})_4(\text{CH}_3)]$ are defined as shown in (XIII) and (XIV). The bond angles and dipole moment derivatives for $[\text{Mn}(\text{CO})_5(\text{CH}_3)]$ and $[\text{Mn}(\text{CO})_4(\text{CH}_3)]$ are defined as shown in (XV) and (XVI).



(XV)



(XVI)

We thank D. J. Taylor for assistance with the energy-factored CO force-field calculations and the S.R.C. for support (to A. J. R.) and for a Research Studentship (to T. M. M.). We also thank the referees for constructive criticisms and helpful comments.

[9/742 Received, 14th May, 1979]

REFERENCES

- 1 A. Wojcicki, *Adv. Organometallic Chem.*, 1973, **11**, 87.
- 2 K. Noack and F. Calderazzo, *J. Organometallic Chem.*, 1967, **10**, 101.
- 3 F. Calderazzo and F. A. Cotton, *Inorg. Chem.*, 1962, **1**, 30.
- 4 R. J. Mawby, F. Basolo, and R. G. Pearson, *J. Amer. Chem. Soc.*, 1964, **86**, 3994.
- 5 M. Green and D. C. Wood, *J. Amer. Chem. Soc.*, 1966, **88**, 4106.
- 6 K. Noack, M. Ruch, and F. Calderazzo, *Inorg. Chem.*, 1968, **7**, 345.
- 7 C. S. Kraihanzel and P. K. Maples, *Inorg. Chem.*, 1968, **7**, 1806.

- 8 C. S. Kraihanzel and P. K. Maples, *J. Amer. Chem. Soc.*, 1965, **87**, 5267.
- 9 R. F. Heck, *Accounts Chem. Res.*, 1969, **2**, 10.
- 10 R. M. Krupka, H. Kaplan, and K. J. Laidler, *Trans. Faraday Soc.*, 1966, **62**, 2754.
- 11 C. P. Casey, C. A. Bunnell, and J. C. Calabrese, *J. Amer. Chem. Soc.*, 1976, **98**, 1166.
- 12 J. K. Burdett and J. J. Turner, in 'Cryochemistry,' eds. M. Moskovits and G. A. Ozin, John Wiley, London, 1976.
- 13 A. J. Rest and J. R. Sodeau, *J.C.S. Chem. Comm.*, 1975, 696; T. M. McHugh, A. J. Rest, and J. R. Sodeau, *J.C.S. Dalton*, 1979, 184.
- 14 A. J. Rest, *J. Organometallic Chem.*, 1970, **25**, C30.
- 15 M. M. Rochkind, *Spectrochim. Acta*, 1971, **A27**, 547.
- 16 T. M. McHugh, Ph.D. Thesis, University of Southampton, 1980.
- 17 R. B. King, 'Organometallic Syntheses,' eds. J. J. Eisch and R. B. King, Academic Press, London, 1965, vol. 1, p. 147.
- 18 H. M. Seip and R. Seip, *Acta Chem. Scand.*, 1970, **24**, 3431.
- 19 P. S. Braterman, 'Metal Carbonyl Spectra,' Academic Press, London, 1975.
- 20 A. J. Downs and S. C. Peake, in 'Molecular Spectroscopy,' *Specialist Periodical Reports*, The Chemical Society, London, 1973, **1**, 523.
- 21 T. M. McHugh, A. J. Rest, and D. J. Taylor, *J.C.S. Dalton*, 1980, 1803.
- 22 H. D. Kaesz, R. Bau, D. Hendrickson, and J. M. Smith, *J. Amer. Chem. Soc.*, 1967, **89**, 2844.
- 23 G. Keeling, S. F. A. Kettle, and I. J. Paul, *J. Chem. Soc. (A)*, 1971, 3143.
- 24 G. B. Blakney and W. F. Allen, *Inorg. Chem.*, 1971, **10**, 2763.
- 25 A. J. Rest and D. J. Taylor, *J.C.S. Chem. Comm.*, 1977, 717.
- 26 B. A. Frenz, J. H. Enemark, and J. A. Ibers, *Inorg. Chem.*, 1969, **8**, 1288.
- 27 R. N. Perutz and J. J. Turner, *J. Amer. Chem. Soc.*, 1975, **97**, 4800.
- 28 M. Poliakoff, *J.C.S. Faraday II*, 1977, 569.
- 29 J. K. Burdett, M. A. Graham, R. N. Perutz, M. Poliakoff, A. J. Rest, J. J. Turner, and R. F. Turner, *J. Amer. Chem. Soc.*, 1975, **97**, 4805.
- 30 O. Crichton, M. Poliakoff, A. J. Rest, and J. J. Turner, *J.C.S. Dalton*, 1973, 1321.
- 31 J. F. Ogilvie, *Chem. Comm.*, 1970, 323.
- 32 R. B. King, A. D. King, jun., M. Z. Iqbal, and C. C. Frazier, *J. Amer. Chem. Soc.*, 1978, **100**, 1687.
- 33 M. Poliakoff, *Inorg. Chem.*, 1976, **15**, 2022.
- 34 D. J. Darensbourg and B. J. Baldwin, *J. Amer. Chem. Soc.*, 1979, **101**, 6447.
- 35 R. S. Berry, *J. Chem. Phys.*, 1960, **32**, 933.
- 36 M. Poliakoff, *Inorg. Chem.*, 1976, **15**, 2892.
- 37 D. J. Darensbourg and G. R. Dobson, *J. Organometallic Chem.*, 1976, **116**, C17.
- 38 J. D. Attwood and T. L. Brown, *J. Amer. Chem. Soc.*, 1975, **97**, 3380.
- 39 D. L. Lichtenberger and T. L. Brown, *J. Amer. Chem. Soc.*, 1978, **100**, 366.
- 40 H. Berke and R. Hoffmann, *J. Amer. Chem. Soc.*, 1978, **100**, 7224.
- 41 T. C. Flood and J. E. Jensen, Proceedings of the International Conference on Organometallic Chemistry, Dijon, 1979, paper D34.
- 42 G. Facinetti and C. Floriani, *J.C.S. Chem. Comm.*, 1972, 654; G. Facinetti, G. Fochi, and C. Floriani, *J.C.S. Dalton*, 1977, 1946.
- 43 G. Erker and F. Rosenfeldt, *Angew. Chem. Internat. Edn.*, 1978, **17**, 605.
- 44 E. C. Guzman, G. Wilkinson, J. L. Atwood, R. D. Rogers, W. E. Hunter, and M. J. Zaworotko, *J.C.S. Chem. Comm.*, 1978, 465.
- 45 J. M. Manriquez, D. R. McAlister, R. D. Sanner, and J. E. Bercaw, *J. Amer. Chem. Soc.*, 1978, **100**, 2716.
- 46 J. M. Manriquez, P. J. Fagan, T. J. Marks, C. S. Day, and V. W. Day, *J. Amer. Chem. Soc.*, 1978, **100**, 7112.
- 47 T. C. Brown and P. A. Bellus, *Inorg. Chem.*, 1978, **17**, 3726.
- 48 A. J. Rest and J. J. Turner, *Chem. Comm.*, 1969, 375.
- 49 M. Poliakoff, J. A. Timney, and J. J. Turner, Proceedings of the IXth International Conference on Organometallic Chemistry, Dijon, 1979, paper D5.
- 50 M. Poliakoff, personal communication.